Biochemical and Biophysical Research Communications 393 (2010) 168–173

Contents lists available at ScienceDirect

Biochemical and Biophysical Research Communications

journal homepage: www.elsevier.com/locate/ybbrc

The C-terminal regulatory domain is required for catalysis by *Neisseria meningitidis* α-isopropylmalate synthase

Frances H.A. Huisman [a,b], Michael F.C. Hunter [a,b], Sean R.A. Devenish [a,c,1], Juliet A. Gerrard [a,c], Emily J. Parker [a,b,*]

[a] Biomolecular Interaction Centre, University of Canterbury, Christchurch, New Zealand
[b] Department of Chemistry, University of Canterbury, Christchurch, New Zealand
[c] School of Biological Sciences, University of Canterbury, Christchurch, New Zealand

ARTICLE INFO

Article history:
Received 25 January 2010
Available online 1 February 2010

Keywords:
α-IPMS
Regulatory domain
Allosteric regulation
Leucine biosynthesis
Neisseria meningitidis

ABSTRACT

α-Isopropylmalate synthase (α-IPMS) catalyses the first committed step in leucine biosynthesis in many pathogenic bacteria, including *Neisseria meningitidis*. This enzyme (*Nme*IPMS) has been purified, characterised, and compared to α-IPMS proteins from other bacteria. *Nme*IPMS is a homodimer which catalyses the condensation of α-ketoisovalerate (α-KIV) and acetyl coenzyme A (AcCoA), and is inhibited by leucine. *Nme*IPMS can use alternate α-ketoacids as substrates and, in contrast to α-IPMS from other sources, is activated by a range of metal ions including Cd^{2+} and Zn^{2+} that have previously been reported as inhibitory, since they suppress the dithiodipyridone assay system rather than the enzyme itself. Previous studies indicate that α-IPMS is a TIM barrel enzyme with an allosteric leucine-binding domain. To assess the importance of this domain, a truncated form of *Nme*IPMS was generated and characterised. Loss of the regulatory domain resulted in a loss of the ability to catalyse the aldol reaction, although the enzyme was still able to slowly hydrolyse AcCoA independently of α-KIV at a rate similar to that of the WT enzyme. This implies that the regulatory domain is not only required for control of enzymatic activity but may assist in the positioning of key residues in the catalytic TIM barrel. The importance of this domain to catalytic function may offer new strategies for inhibitor design.

Introduction

Whereas mammals utilise environmental supplies of the branched-chain amino acids, leucine, isoleucine and valine, many bacteria and plants have enzymes for *de novo* synthesis of these compounds. Several studies have shown that *Mycobacterium bovis* requires the leucine biosynthetic pathway for survival inside mice and host macrophages [1]. In addition, *Corynebacterium glutamicum*, *Salmonella typhimurium*, and *Neurospora crassa* exhibited leucine auxotrophy when this pathway was disrupted [2,3]. These enzymes are therefore potential targets for inhibition, as inhibitors may be antibacterial with limited host toxicity. Despite this potential, the branched-chain amino acid pathway is amongst the least studied of the amino acid biosynthetic pathways.

α-Isopropylmalate synthase (α-IPMS, EC 2.3.3.13) catalyses the first committed step in leucine biosynthesis (Fig. 1), the condensation reaction between α-ketoisovalerate (α-KIV) and acetyl coenzyme A (AcCoA) to form (*S*)-α-isopropylmalate (α-IPM). This enzyme belongs to the Claisen-condensing family, along with malate synthase, citrate synthase, and homocitrate synthase. α-IPMS is feedback inhibited by the end product of its pathway, leucine, in organisms such as *Mycobacterium tuberculosis* [4] and *S. typhimurium* [5].

Previous studies of α-IPMS have been limited to few organisms, including *S. typhimurium* [6,7], *C. glutamicum* [2], and *M. tuberculosis* [4,8–13]. The most in-depth biochemical studies and only known crystal structures are of the α-IPMS from *M. tuberculosis* (*Mtu*IPMS) [9].

*Mtu*IPMS is a homodimer of two 70 kDa monomers both in solution and in the crystalline form [9]. Other α-IPMS variants such as the enzyme from *S. typhimurium* have been reported to form tetramers [6]. Each monomer of *Mtu*IPMS is composed of a $(\beta/\alpha)_8$ TIM barrel and a regulatory domain of novel fold, separated by a flexible linker domain. α-KIV and a Zn^{2+} ion bind at the C-terminal end

Abbreviations: α-IPMS, α-isopropylmalate synthase; α-KIV, α-ketoisovalerate; AcCoA, acetyl coenzyme A; α-IPM, (*S*)-α-isopropylmalate; *Mtu*IPMS, *M. tuberculosis* α-IPMS; *Nme*IPMS, *N. meningitidis* α-IPMS; (*S*)-α-HIV, (*S*)-α-hydroxyisovalerate; WT, wild-type; DTP, 4,4′-dithiodipyridone; DSF, differential scanning fluorimetry; BTP, bis–tris-propane

* Corresponding author. Address: Department of Chemistry, University of Canterbury, Private Bag 4800, Christchurch, New Zealand. Fax: +64 3 364 2110.
E-mail address: emily.parker@canterbury.ac.nz (E.J. Parker).
[1] Present address: Department of Biochemistry, University of Cambridge, Cambridge, UK.

0006-291X/$ - see front matter © 2010 Elsevier Inc. All rights reserved.
doi:10.1016/j.bbrc.2010.01.114

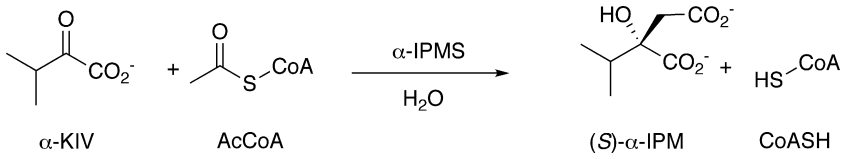

Fig. 1. Reaction catalysed by α-IPMS.

of the TIM barrel, and modelling studies imply AcCoA binds in a large pocket on the *Re* face of α-KIV. Leucine binds the C-terminal regulatory domain [9]. Two residues from one monomer (His379 and Tyr410) protrude into the active site of the other, and may play a key role in allosteric regulation. It has been shown recently that mutation of Tyr410 to phenylalanine negates all leucine-induced inhibition, without preventing leucine from binding in the regulatory domain [4]. Several point mutations and a deletion of part of the regulatory domain of the *Saccharomyces cerevisiae* α-IPMS results in insensitivity to leucine [14]. However, the role of the entire regulatory domain has never been probed. This is intriguing, as inspection of the sequence databases indicates that several annotated α-IPMS enzymes appear to be 'naturally truncated', lacking a complete C-terminal regulatory domain, such as some forms from *Staphylococcus aureus* and *Francisella tularensis*.

The *Mtu*IPMS enzyme shows Zn^{2+} bound near the active site, coordinating the carbonyl functionalities of α-KIV, thereby orienting the substrate and polarising the ketone for reaction [9]. All α-IPMS enzymes require a divalent metal for activity and some enzymes also display dependency on a monovalent cation [10].

Neisseria meningitidis is a human pathogen, able to infect the respiratory system or larynx, and can also infect the blood causing fatal septicaemia. This organism is best known for causing bacterial meningitis, leading to brain damage or even death. In this study we describe the expression and purification of *N. meningitidis* α-IPMS (*Nme*IPMS), and the characterisation of the enzyme with respect to metal dependency, leucine inhibition, and substrate specificity. A truncated mutant, lacking the regulatory domain, was also generated and found to be catalytically compromised. This study highlights several common features between *Nme*IPMS and *Mtu*IPMS, and also illuminates some significant differences in their inhibition by leucine.

Materials and methods

Cloning. The *leuA* gene was amplified from *N. meningitidis* MC58 (serogroup B) genomic DNA (ATCC) (primer information in Supplementary Material). A TOPO-cloning kit (Invitrogen) was used to ligate the resulting 1.5 kbp PCR product into a pET-151 vector. Plasmid was transformed into chemically competent *Escherichia coli* OneShot TOP10 cells, plasmid DNA was purified, and the sequence was verified.

Quikchange site-directed mutagenesis was used to insert a stop codon at residue Glu365, chosen as it is upstream of the regulatory domain, not highly conserved and is located in undefined loop of the *Mtu*IPMS structure. Plasmids containing the *leuA* gene and the truncated version were transformed into chemically competent *E. coli* BL21(DE3)Star cells for expression.

Purification. WT and E365Term *Nme*IPMS were expressed and purified using identical protocols. *E. coli* BL21(DE3)Star cells containing the desired plasmid were grown overnight in ZYM-5052 auto-inducing media at 37 °C [15]. Cells were harvested by centrifugation at 4700*g* for 30 min, and resuspended in Buffer A (50 mM potassium phosphate, 300 mM KCl, pH 8.0). Cells were lysed by sonication. The soluble fraction was separated by centrifugation at 12,000*g* for 30 min and passed through 5 mL Talon Superflow Metal Affinity resin. The resin was washed with Buffer A, and protein eluted with Buffer B (Buffer A plus 150 mM imidazole, pH 8.0). Protein-containing fractions were desalted, and DTT (1 mM) and EDTA (0.5 mM) were added. The His-tag was cleaved by overnight incubation at 4 °C with TEV protease [16]. TEV protease and cleaved His-tag were removed from solution using Talon Superflow Metal Affinity resin, and the protein-containing fractions pooled and further purified by anion exchange chromatography on a SourceQ column using 25 mM bis–tris-propane (BTP) buffer (pH 7.0) and a linear gradient of KCl. Enzyme-containing fractions were identified by gel electrophoresis as a major band, which corresponded well with the calculated molecular weights of 56 and 40 kDa for WT and E365Term, respectively, then pooled and stored at −80 °C at 5–10 mg/mL.

Dithiodipyridone-coupled assay at 324 nm. Initial velocity data were obtained using 4,4′-dithiodipyridone (DTP) to detect the formation of CoASH product at 324 nm, (ε of 1.98×10^4 L/mol cm) at 25 °C. A typical reaction involved an assay solution containing 80 μM AcCoA, 500 μM α-KIV, 100 μM DTP, 20 mM KCl, and 20 mM $MgCl_2$ in 1 mL of 50 mM HEPES (pH 7.5) in a quartz cuvette, brought to temperature, and initiated by addition of purified WT enzyme to a concentration of 10 nM. Assays investigating uncoupled hydrolysis used no α-KIV, and an increased WT protein concentration of 3.3 μM. Assays using E365Term contained a higher AcCoA concentration of 500 μM, and were initiated with 2.5 μM enzyme. All kinetic measurements were performed in duplicate, and typical error was less than 10%. Apparent K_m data were determined by fitting to the Michaelis–Menten equation, and inhibition data were fitted to either a competitive or mixed inhibition model using Grafit [17].

Direct assay at 232 nm. Direct assays were carried out as described above for the DTP assay, substituting 50 mM BTP for HEPES and omitting DTP. Changing metal concentration and pH caused significant variation in abs(AcCoA)–abs(CoASH), so every assay solution was calibrated using known concentrations (of the order of 16 μM) of CoASH and AcCoA.

Gel filtration chromatography. The multimeric states of WT and E365Term proteins were determined by gel filtration chromatography using a Superdex 200 10/300 GL column (GE Healthcare). Samples (500 μL, 2 mg/mL) and standards (Sigma) were run in 50 mM Tris–HCl (pH 7.5) with 100 mM KCl. WT enzyme was also run in the presence of 200 μM leucine.

Differential scanning fluorimetry. Differential scanning fluorimetry (DSF) was carried out using a BioRad iCycler iQ5 Multicolour Real-Time PCR Detection System. SYBROrange dye was added to a protein and ligand mixture in a 96-well plate. This sealed plate was subjected to a thermal melt program from 20 to 95 °C in 0.2 °C increments over 4 h. Each sample was measured in triplicate and compared to a control containing ligand solution and dye, but no protein. Melting temperatures were determined as the temperature at which the greatest increase in fluorescence was measured.

Metal dependency. Residual metal from purification was removed by dialysing 2 mL of 2 mg/mL enzyme at 4 °C against 250 mL of 50 mM BTP (pH 7.5), 300 mM KCl, and 250 mM EDTA for 4 h, then against 250 mL of 50 mM BTP (pH 7.5), 300 mM KCl, and 100 μM EDTA for 4 h, with the buffer being changed at 2 h. Metal reactivation was measured using the DTP assay with $MgCl_2$

replaced by various concentrations of the relevant metal as the dichloride. Rates in the presence of Cd^{2+} and Zn^{2+} were measured using the 232 nm assay.

Substrate analogue testing. Activity was measured according to standard assay conditions with the substrate analogue replacing α-KIV. Compounds inactive as substrates had their inhibitory parameters determined using standard assay conditions modified to contain varying concentrations of inhibitor and substrate. Reactions were initiated with enzyme.

CoASH inhibition. CoASH inhibition was tested using a standard 232 nm assay, containing varying concentrations of CoASH and initiated with AcCoA instead of enzyme after 2 min of incubation (80 μM AcCoA). Time-dependence of CoASH inhibition was measured by determining the activity of preincubated *Nme*IPMS (0.2 mg/mL in 50 mM BTP (pH 7.5) and 30 mM KCl) with concentrations of up to 1.2 mM CoASH for up to 20 min.

Leucine inhibition. Leucine inhibition was examined using the standard DTP assay, with 250 μM AcCoA and α-KIV and leucine concentrations from 0 to 200 μM. pH dependence of leucine inhibition was measured for WT enzyme at 232 nm, using 100 μM AcCoA and 250 μM α-KIV. Assays were carried out in BTP buffer at pH 6.5, 7.5, or 8.5 with leucine concentrations of 0–2 mM.

Results

Cloning and isolation

The sequence of the cloned WT gene was consistent with that encoding α-IPMS from *N. meningitidis* (NCBI Gene ID: 903489). A mutant lacking the regulatory domain, E365Term, was generated using site-directed mutagenesis to introduce a stop codon in place of residue Glu365, upstream of the C-terminal regulatory domain. This mutation was confirmed by sequencing and by the reduced size of the expressed protein.

WT and mutant proteins were expressed and purified to homogeneity by a combination of immobilised metal affinity and anion exchange chromatography. The tag was cleaved, leaving the protein with an N-terminal GIDPFT extension. The calculated molecular masses of 56,027 and 39,931 Da, for the purified WT and E365Term proteins, respectively, corresponded well with the masses seen by SDS–PAGE (Supplementary Material, Fig. S1).

Size exclusion chromatography indicated that both WT and E365Term proteins are homodimeric. The presence of leucine had no effect on oligomeric state.

Stability

Differential scanning fluorimetry (DSF) was used to investigate the thermal stability of *Nme*IPMS in combination with various additives (Fig. 2). WT protein denatured at 44.5 ± 0.4 °C, and this increased to 59 ± 3 °C in the presence of leucine. This stabilisation was not observed with valine or glycine. WT protein was also stabilised by α-KIV, an effect that is cumulative with leucine stabilisation. Interestingly, E365Term showed similar stability to WT *Nme*IPMS, but exhibited no increased stability in the presence of AcCoA, α-KIV or leucine. Circular dichroism spectroscopy confirmed the melting temperature of WT *Nme*IPMS, and that E365Term *Nme*IPMS adopted a similar secondary structure to that of WT enzyme (Figs. S2 and S3, Supplementary Material).

Kinetic characterisation

Kinetic assays were carried out using a DTP-coupled assay, monitoring absorbance at 324 nm to follow the generation of a thio-pyridone by reaction of DTP with the enzyme reaction product CoASH [10]. However, this assay method was not suitable for all kinetic determinations as certain conditions cause the CoASH + DTP reaction to become rate limiting, such as high pH (>8.0) or the presence of Zn^{2+}, Cd^{2+} or CoASH. In these cases the enzyme-catalysed reaction was followed by monitoring the loss of AcCoA at 232 nm.

Using the DTP-coupled assay, K_m values for WT *Nme*IPMS were determined to be 30 ± 2 and 35 ± 3 μM for α-KIV and AcCoA, respectively. These values are somewhat different from those reported for *Mtu*IPMS (12 ± 1 μM for α-KIV and 136 ± 5 μM for AcCoA [11]). The k_{cat} for WT *Nme*IPMS was found to be 13 ± 0.3 s^{-1}, compared with k_{cat} values of 3.5 ± 0.1 and 2.1 ± 0.1 s^{-1} reported for *Mtu*IPMS [11]. WT *Nme*IPMS also catalysed uncoupled hydrolysis of AcCoA in the absence of α-KIV, with a K_m of 250 ± 30 μM and a k_{cat} of 0.011 ± 0.001 s^{-1}. WT *Nme*IPMS activity was shown to vary with pH, with maximal activity observed at pH 8.5 (Supplementary Material, Fig. S4), and the thermal optimum of the enzyme was found to be 40 °C (Supplementary Material, Fig. S5).

The rate of the *Nme*IPMS-catalysed reaction was greatly reduced in the truncated mutant, to the extent that the rate of uncoupled AcCoA hydrolysis obscured any condensation reaction. AcCoA had a K_m of 150 ± 20 μM for uncoupled hydrolysis, with a k_{cat} of 0.010 ± 0.001 s^{-1}. This rate increased by 40% in the presence of 500 μM α-KIV.

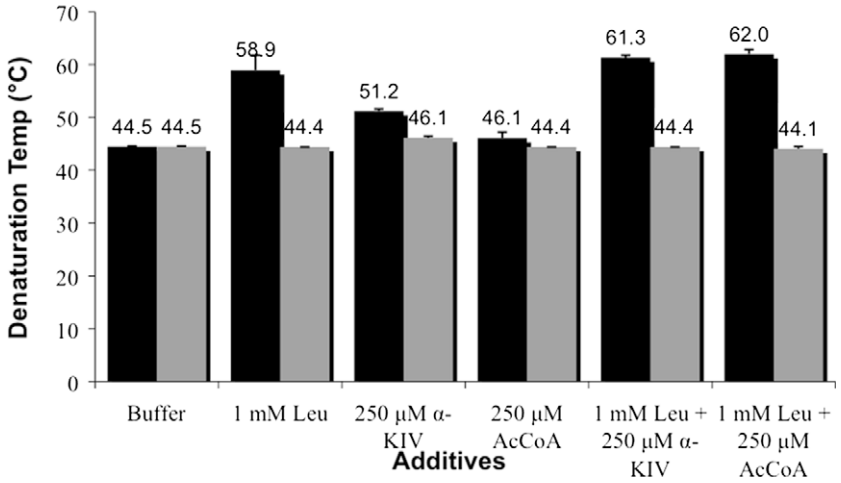

Fig. 2. Denaturation temperature of WT (black) and E365Term (grey) *Nme*IPMS in the presence of substrates and allosteric inhibitor. All solutions contained 25 mM BTP buffer (pH 7.0) and 0.16 mg/mL protein.

Metal dependence

Dialysis against EDTA led to a 30-fold drop in activity compared to freshly purified *Nme*IPMS, indicating a strong divalent metal dependency. In the presence of Zn^{2+} or Cd^{2+}, addition of CoASH to DTP failed to give an increase in absorbance at 324 nm in control experiments, so the direct assay at 232 nm was used in the presence of these metals (Fig. 3).

With the exception of Mg^{2+}, all metals have optimum activating concentrations below 0.2 mM and show significant loss of activity at higher concentrations. Mn^{2+} and Co^{2+} show strong activation, whereas Ni^{2+}, Cd^{2+}, and Zn^{2+} are all weakly activating. Mg^{2+} is distinctive in that it requires much higher concentrations to activate the enzyme, but also shows no reduced effect at concentrations up to 20 mM. Also, unlike the other metals tested, except Cd^{2+}, it does not cause a large increase in stability of *Nme*IPMS as measured by DSF (Table S1, Supplementary Material). The metal dependency profile for *Nme*IPMS differs considerably from that observed for *Mtu*IPMS, for which Zn^{2+} and Cd^{2+} were characterised as inhibitors, and Mn^{2+}, Co^{2+}, and Ni^{2+} all showed activation curves similar to Mg^{2+} [10]. In contrast to some forms of α-IPMS that are activated by monovalent ions, *Nme*IPMS activity was not enhanced by either KCl or NaCl (up to 20 mM). It should be noted that even the best specific activity attained was not as high as the activity before dialysis, suggesting some activity is lost during the dialysis process.

Substrate analogue testing

A variety of ketoacids were tested as substrates for WT *Nme*IPMS (Table 1). An unbranched side chain, as in α-ketobutyrate and α-ketopropanoate, causes a higher K_m but comparable k_{cat}, whereas shortening it, as in pyruvate and 3-fluoropyruvate, raises K_m and lowers k_{cat}. All of these are substrates for *Mtu*IPMS other than 3-fluoropyruvate (which has not been tested for this enzyme) [11,18].

Analogues that were not substrates were tested for inhibition. Several analogues were weak inhibitors, whilst 3-bromopyruvate, 3,3-dibromopyruvate and (*S*)-α-hydroxyisovalerate ((*S*)-α-HIV) exhibited reversible, competitive inhibition with respect to α-KIV (Table 2). (*S*)-α-HIV can be understood as a transition state analogue of the putative alkoxide intermediate, whereas the first two seem to gain strong (but unreactive) binding affinity from their halogens.

CoASH inhibition

Using the direct assay, product CoASH was determined not to be an inhibitor of WT *Nme*IPMS. Time dependent inactivation by

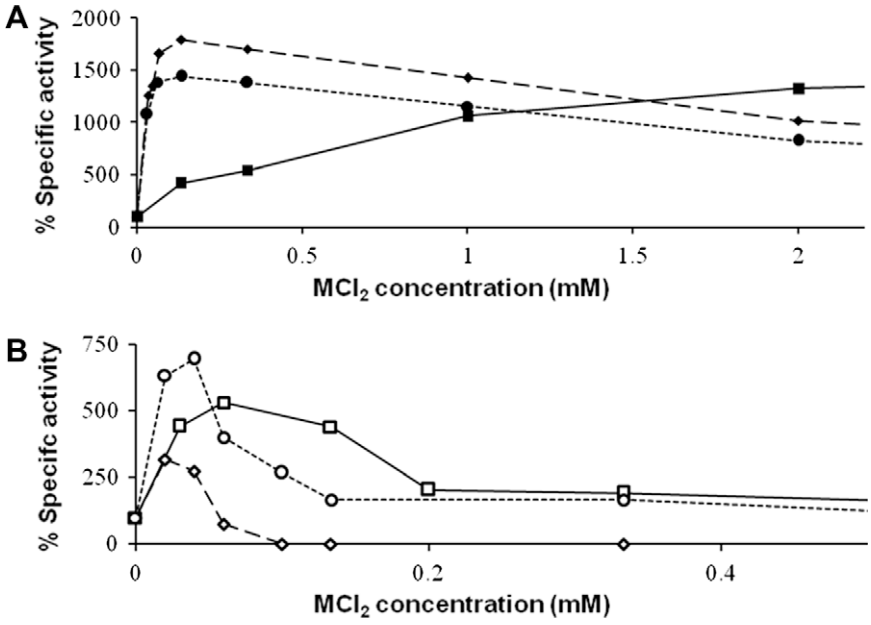

Fig. 3. Steady state kinetics for specific activity of dialysed *Nme*IPMS by divalent metals provided as the dichloride. Specific activity is relative to dialysed *Nme*IPMS with no divalent metal added. (A) Activation by Mg^{2+} (–■–), Mn^{2+} (–▲–) and Co^{2+} (··●··). (B) Activation by Ni^{2+} (–□–), Cd^{2+} (–△–) and Zn^{2+} (··○··).

Table 1
Activities of alternate substrates. Assays performed in 50 mM HEPES (pH 7.5), 20 mM $MgCl_2$, 80 μM AcCoA, and 0.6 mM KCl at 25 °C. Dialysed enzyme was used.

Substrate	K_m (mM)	k_{cat} (s^{-1})	Substrate	K_m (mM)	k_{cat} (s^{-1})
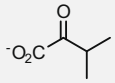	0.035 ± 0.002	5.4 ± 0.1	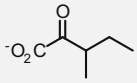	0.28 ± 0.03	0.027 ± 0.001
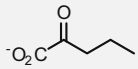	0.62 ± 0.07	3.4 ± 0.1		1.5 ± 0.3	0.63 ± 0.04
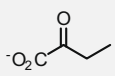	1.36 ± 0.06	3.3 ± 0.4	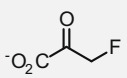	105 ± 20	0.3 ± 0.1

Table 2
Inhibition of *Nme*IPMS by α-KIV analogues. * Indicates weak inhibition observed (IC_{50} of above 1 mM in the presence of 100 μM α-KIV). ND indicates no inhibitory activity detected at 1 mM.

Inhibitor	K_i (mM)	Inhibitor	K_i (mM)
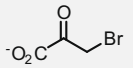	0.06 ± 0.03	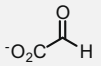	*
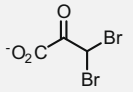	0.03 ± 0.02	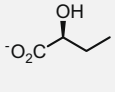	*
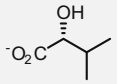	2.5 ± 1	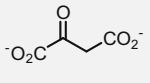	*
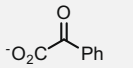	ND	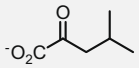	*
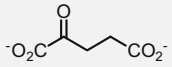	ND		

CoASH, as observed for *Saccharomyces cerevisiae* α-IPMS [19] was not observed for *Nme*IPMS.

Allosteric inhibition

Allosteric inhibition of WT enzyme by leucine fits a mixed, non-competitive model with respect to both α-KIV and AcCoA (Table 3). Inhibition of WT catalytic activity is specific to leucine; similar amino acids (valine, glycine) had no effect. Uncoupled hydrolysis of AcCoA was unaffected by leucine in both the WT and E365Term enzymes.

de Carvalho et al. found that, in the presence of leucine, reactions catalysed by *Mtu*IPMS showed an initial burst of product formation, followed by a slower, linear rate [8]. No such time-dependent inhibition was observed for WT *Nme*IPMS (Fig. S6, Supplementary Material).

WT *Nme*IPMS was far more sensitive to leucine at pH 6.5 than at pH 8.5. Inhibitor at 200 μM caused a loss of 20% activity at pH 8.5, 54% loss at pH 7.5 and 89% loss at pH 6.5, whereas 2 mM inhibitor reduced activity by 50%, 81%, and 95% at pH 8.5, 7.5, and 6.5, respectively. pH dependence was also shown for α-IPMS from *S. typhimurium* [6], which was found to be 30-fold more sensitive to leucine inhibition at pH 6.5 than at pH 8.5.

Discussion

Active WT *Nme*IPMS was heterologously expressed and purified from *E. coli*. In general, this enzyme exhibits similar properties to other characterised α-IPMS enzymes, having comparable kinetic parameters, a tolerance for alternative α-ketoacid substrates, a preference for alkaline pH for maximal activity, and a dimeric quaternary structure. As with most other forms of α-IPMS that have been characterised to date, *Nme*IPMS displays activation by divalent metals. In contrast, only Mg^{2+} shows simple saturation kinetics for *Nme*IPMS, whilst other divalent metals have distinct activity maxima, and are less activating at concentrations greater than 200 μM. Zn^{2+} and Cd^{2+} were characterised as strongly inhibitory in previous studies [10,13]; however, these results could be artefactual, caused by these ions suppressing the DTP dependent assay. Using the direct assay these metals are modest activators of *Nme*IPMS. *Nme*IPMS shows no activation by monovalent cations at any concentration, whereas a strong correlation between monovalent cation concentration and activity has been reported for *Mtu*IPMS, although *Mtu*IPMS has no obvious binding site for such a cation.

Sequence alignments show that *Mtu*IPMS and *Nme*IPMS share all key residues associated with the binding of α-KIV. It is therefore unsurprising that they both tolerate similar changes to substrate α-KIV. Whilst pyruvate is a poor substrate, introduction of a 3-fluoro substituent increases K_m 70-fold, and a 3-bromo substitution converts pyruvate into a potent reversible inhibitor. This suggests that bromine is a good fit for the side chain pocket of the enzyme, unlike the significantly smaller fluorine. The three nearest residues to the α-KIV side chain are the polar His99, Ser131, and Asn159, possibly supporting the binding of modestly polar bromo substituent compared to the nonpolar isopropyl group of α-KIV.

In common with many other enzymes that catalyse the first committed step in a biosynthetic pathway, α-IPMS is inhibited by the pathway end product, leucine. For *Nme*IPMS this inhibition pattern does not show the unusual time-dependency that was observed for *Mtu*IPMS, indicating that there is some variation in the nature of allosteric regulation between enzymes from different sources. The structure of *Mtu*IPMS indicates that catalysis is mediated by the $(\beta/\alpha)_8$ barrel domain and, as for many other $(\beta/\alpha)_8$ barrel containing enzymes, α-IPMS has an accessory domain that is associated with regulation. Intriguingly, a truncated *Nme*IPMS, lacking the allosteric domain, was unable to catalyse the aldol reaction, indicating that catalytic and regulatory functions of this enzyme cannot be readily uncoupled. In an earlier study, protease treatment gave a *Mtu*IPMS truncated at both the N-terminal and C-terminal ends, reportedly giving an active barrel core, although it is unclear whether uncoupled AcCoA hydrolysis was assessed [13]. In contrast, our engineered *Nme*IPMS mutant catalysed only the uncoupled hydrolysis of AcCoA, a reaction that was over 1000 times slower than the aldol reaction catalysed by the wild-type enzyme.

Uncoupling of regulatory and catalytic sites has been achieved recently for *Mtu*IPMS, where a point mutation Y410F created a leucine insensitive variant [4]. The activity of this protein was considerably compromised, however, giving a maximum catalytic rate (~3% of wild-type enzyme) lower than the reported rate for the maximally inhibited enzyme (10%). The equivalent residue (Tyr313) and the structural element bearing it were deliberately retained in the engineered *Nme*IPMS truncation. It appears likely that the regulatory domain assists in optimal positioning of this key residue and supports the active site structure for the uninhibited enzyme. It would be interesting to resolve how the active site is supported in α-IPMS enzymes that are 'naturally truncated'. It is also interesting to note that there are closely related enzymes catalysing similar reaction chemistry that share a homologous barrel structure and active site architecture, including the recently identified *Re*-citrate synthase from *Clostridium kluyveri* [20] and the aldolase portion of the bifunctional enzyme 4-hydroxy-2-ketovalerate aldolase/acylating acetaldehyde dehydrogenase [21]. Although *Re*-citrate synthase is yet to be structurally characterised, these enzymes clearly display significant variation in their extra barrel regions. The observation that an intact regulatory domain is critical to support catalytic function of *Nme*IPMS may enable inhibitor design targeted specifically at this enzyme.

Table 3
Leucine inhibition of WT *Nme*IPMS with respect to AcCoA and α-KIV, compared with inhibition of *Mtu*IPMS with respect to α-KIV.

	Inhibition constants (μM)		
	Nme		*Mtu* [8]
	AcCoA	α-KIV	α-KIV
K_i	8 ± 1	57 ± 23	22 ± 2
K_i'	52 ± 17	18 ± 2	8 ± 1

Acknowledgments

This work is supported by the Maurice Wilkins Centre for Molecular Biodiscovery. S.R.A.D. thanks the Foundation for Research, Science and Technology for postdoctoral funding (Contract UOCX0603).

Appendix A. Supplementary data

Supplementary data associated with this article can be found, in the online version, at doi:10.1016/j.bbrc.2010.01.114.

References

[1] F.C. Bange, A.M. Brown, W.R. Jacobs, Leucine auxotrophy restricts growth of *Mycobacterium bovis* BCG in macrophages, Infect. Immun. 64 (1996) 1794–1799;
R.A. McAdam, T.R. Weisbrod, J.L. Martin, J.D. Scuderi, A.M. Brown, J.D. Cirillo, B.R. Bloom, W.R. Jacobs, *In vivo* growth characteristics of leucine and methionine auxotrophic mutants of *Mycobacterium bovis* BCG generated by transposon mutagenesis, Infect. Immun. 63 (1995) 1004–1012.

[2] M. Pátek, K. Krumbach, L. Eggeling, H. Sahm, Leucine synthesis in *Corynebacterium glutamicum*: enzyme activities, structure of leuA, and effect of leuA inactivation on lysine synthesis, Appl. Environ. Microbiol. 60 (1994) 133–140.

[3] C. Jungwirth, S.R. Gross, P. Margolin, H.E. Umbarger, The biosynthesis of leucine. I. The accumulation of β-carboxy-β-hydroxyisocaproate by leucine auxotrophs of *Salmonella typhimurium* and *Neurospora crassa*, Biochemistry 2 (1963) 1–6.

[4] L.P. de Carvalho, P. Frantom, A. Argyrou, J. Blanchard, Kinetic evidence for inter-domain communication in the allosteric regulation of α-isopropylmalate synthase from *Mycobacterium tuberculosis*, Biochemistry (2009).

[5] E. Teng-Leary, G.B. Kohlhaw, Mechanism of feedback inhibition by leucine. Binding of leucine to wild-type and feedback-resistant α-isopropylmalate synthases and its structural consequences, Biochemistry 12 (1973) 2980–2986.

[6] G.B. Kohlhaw, T.R. Leary, H.E. Umbarger, α-Isopropylmalate synthase from *Salmonella typhimurium*. Purification and properties, J. Biol. Chem. 244 (1969) 2218–2225.

[7] T.R. Leary, G.B. Kohlhaw, α-Isopropylmalate synthase from *Salmonella typhimurium*. Analysis of the quaternary structure and its relation to function, J. Biol. Chem. 247 (1972) 1089–1095.

[8] L.P. de Carvalho, A. Argyrou, J.S. Blanchard, Slow-onset feedback inhibition: inhibition of *Mycobacterium tuberculosis* α-isopropylmalate synthase by L-leucine, J. Am. Chem. Soc. 127 (2005) 10004–10005.

[9] N. Koon, C.J. Squire, E.N. Baker, Crystal structure of LeuA from *Mycobacterium tuberculosis*, a key enzyme in leucine biosynthesis, Proc. Natl. Acad. Sci. USA 101 (2004) 8295–8300.

[10] L.P. de Carvalho, J.S. Blanchard, Kinetic analysis of the effects of monovalent cations and divalent metals on the activity of *Mycobacterium tuberculosis* α-isopropylmalate synthase, Arch. Biochem. Biophys. 451 (2006) 141–148.

[11] L.P. de Carvalho, J.S. Blanchard, Kinetic and chemical mechanism of α-isopropylmalate synthase from *Mycobacterium tuberculosis*, Biochemistry 45 (2006) 8988–8999.

[12] W. Chanchaem, P. Palittapongarnpim, The significance and effect of tandem repeats within the *Mycobacterium tuberculosis* leuA gene on α-isopropylmalate synthase, FEMS Microbiol. Lett. 286 (2008) 166–170.

[13] K. Singh, V. Bhakuni, Cation induced differential effect on structural and functional properties of *Mycobacterium tuberculosis* α-isopropylmalate synthase, BMC Struct. Biol. 7 (2007) 39.

[14] D. Cavalieri, E. Casalone, B. Bendoni, G. Fia, M. Polsinelli, C. Barberio, Trifluoroleucine resistance and regulation of alpha-isopropyl malate synthase in *Saccharomyces cerevisiae*, Mol. Gen. Genet. 261 (1999) 152–160.

[15] F.W. Studier, Protein production by auto-induction in high density shaking cultures, Protein Expr. Purif. 41 (2005) 207–234.

[16] R.B. Kapust, J. Tözsér, J.D. Fox, D.E. Anderson, S. Cherry, T.D. Copeland, D.S. Waugh, Tobacco etch virus protease: mechanism of autolysis and rational design of stable mutants with wild-type catalytic proficiency, Protein Eng. 14 (2001) 993–1000.

[17] R.J. Leatherbarrow, Grafit Version 6, Erithacus Software Ltd., Horly, United Kingdom, 2007.

[18] K. Zhang, M.R. Sawaya, D.S. Eisenberg, J.C. Liao, Expanding metabolism for biosynthesis of nonnatural alcohols, Proc. Natl. Acad. Sci. USA 105 (2008) 20653–20658.

[19] G.B. Kohlhaw, α-Isopropylmalate synthase from yeast, Methods Enzymol. (1988) 414–423.

[20] F. Li, C.H. Hagemeier, H. Seedorf, G. Gottschalk, R.K. Thauer, *Re*-citrate synthase from *Clostridium kluyveri* is phylogenetically related to homocitrate synthase and isopropylmalate synthase rather than to *Si*-citrate synthase, J. Bacteriol. 189 (2007) 4299–4304.

[21] B.A. Manjasetty, J. Powlowski, A. Vrielink, Crystal structure of a bifunctional aldolase-dehydrogenase: sequestering a reactive and volatile intermediate, Proc. Natl. Acad. Sci. USA 100 (2003) 6992–6997.